Article

A positive feedback regulatory loop involving the lncRNA PVT1 and HIF-1α in pancreatic cancer

Yiping Zhu[1], Fang Wu[2], Weiwei Gui[3], Nan Zhang[2], Erik Matro[3], Linghua Zhu[1], Daniel Turunen Eserberg[3], and Xihua Lin ⓘ [2,4,*]

[1] Department of General Surgery, Sir Run Run Shaw Hospital, School of Medicine, Zhejiang University, Hangzhou, China
[2] Department of Endocrinology, Sir Run Run Shaw Hospital, School of Medicine, Zhejiang University, Hangzhou, China
[3] School of Medicine, Zhejiang University, Hangzhou, China
[4] Biomedical Research Center and Key Laboratory of Biotherapy of Zhejiang Province, Sir Run Run Shaw Hospital, Zhejiang University, Hangzhou, China
* Correspondence to: Xihua Lin, E-mail: linxihua@zju.edu.cn

Edited by Hua Lu

Extreme hypoxia is among the most prominent pathogenic features of pancreatic cancer (PC). Both the long non-coding RNA (lncRNA) plasmacytoma variant translocation 1 (PVT1) and hypoxic inducible factor-1α (HIF-1α) are highly expressed in PC patients and play a crucial role in disease progression. Reciprocal regulation involving PVT1 and HIF-1α in PC, however, is poorly understood. Here, we report that PVT1 binds to the HIF-1α promoter and activates its transcription. In addition, we found that PVT1 could bind to HIF-1α and increases HIF-1α post-translationally. Our findings suggest that the PVT1–HIF-1α positive feedback loop is a potential therapeutic target in the treatment of PC.

Introduction

Pancreatic cancer (PC) carries among the worst clinical prognoses of all human cancers. It is the sixth most common cause of adult cancer deaths in China (Zheng et al., 2017) and ranks fourth among cancer-related deaths in the USA (Miller et al., 2019). The overall 5-year survival rate of PC patients is <5% and the median period of disease-free survival (DFS) following radical resection and adjuvant chemotherapy is only 20–22 months (Hidalgo, 2010). Such a poor prognosis is generally considered to be due to a high incidence of metastasis at initial diagnosis, an aggressive disease course and a lack of effective systemic therapies (Hidalgo, 2010). Molecular pathways involved in PC carcinogenesis and progression thus warrant detailed study to uncover novel therapeutic targets for successful treatment.

Long non-coding RNAs (lncRNAs) are defined as non-protein coding transcripts longer than 200 nucleotides. They account for a large proportion of the mammalian genome and play a crucial role in diverse biological processes (Kapranov et al., 2007). A group of lncRNAs were reported to be involved in the pathogenesis of various human malignancies (Bhan et al., 2017). Plasmacytoma variant translocation 1 (PVT1) is a lncRNA encoded by the human PVT1 gene (Webb et al., 1984; Cory et al., 1985). Increased levels of PVT1 expression were reported in a number of human cancers, including gastric (Ding et al., 2014), thyroid (Zhou et al., 2016), and bladder (Zhuang et al., 2015) cancers. PVT1 has also been reported to be overexpressed in PC, and increased levels of PVT1 were associated with more advanced clinical stages and poorer prognoses (Huang et al., 2015). Salivary PVT1 levels have been used as a biomarker for assessing PC patients (Xie et al., 2016). You et al. (2011) reported that inactivation of the PVT1 gene led to enhanced gemcitabine sensitivity in human PC cells. Thus, PVT1 is likely to play a significant role in the pathogenesis of PC.

Previous studies have revealed intra-tumoral hypoxia to be common in the setting of PC and associated with both tumor progression and metastasis (Chen et al., 2016). Hypoxia inducible factor-1 (HIF-1) is a master regulator of cellular adaption to hypoxia and is highly expressed in numerous solid tumors, including PC (Erickson et al., 2015). HIF-1 plays an important role in tumorigenesis, enabling cancer cells to evade the immune system and promoting their proliferation. HIF-1 also contributes to tumor progression by promoting invasion, metastasis, and angiogenesis (Huang, 2013). Structurally, HIF-1 is a heterodimeric transcription factor composed of HIF-1α and HIF-1β

subunits (Hon et al., 2002). HIF-1α is constitutively produced and degrades under normoxic conditions, while HIF-1β expression is unaffected by O_2 levels. Under normoxia, HIF-1α is hydroxylated at specific proline residues (proline 402 and 564) within its O_2-dependent degradation domain by prolyl hydroxylase (Semenza, 2001). Hydroxylated HIF-1α is recognized by the von Hippel-Lindau protein (pVHL), which acts as a ubiquitin E3 ligase. Ubiquitinated HIF-1α subsequently undergoes rapid degradation through the proteasome pathway (Min et al., 2002). The intact HIF-1α translocates to the nucleus, where it heterodimerizes with HIF-1β to bind to hypoxia response elements (HREs) on target genes (Majmundar et al., 2010). A variety of genes are known to be activated at the transcriptional level by HIF-1 in this manner, including EPO, c-Myc, and VEGF (Görlach, 2009). Activation of HIF-1α pathways has been shown to be related to aggressive tumor behavior and poor clinical prognosis (Shih et al., 2017). Detailed study of the regulatory mechanisms involving HIF-1α within cancer cells could thus lead to a better understanding of tumor progression.

Expression of several lncRNAs was reported to be modulated by hypoxia in cancer. Choudhry et al. (2016) first reported hypoxia-responsive lncRNAs as lncRNAs that were upregulated under hypoxia (e.g. H19, lincRNA-p21, linc-ROR, HOTAIR, and NEAT1); others (e.g. ENST00000480739 and lncRNA-LET) were downregulated (Kapinova et al., 2018). Several hypoxia-responsive lncRNAs have been reported to play important roles in HIF-1α pathway regulation and tumorigenesis via modulation of epigenetic changes, transcriptional regulation, and post-transcriptional modification (Shih and Kung, 2017). PVT1 was recently reported to be a direct target of HIF-1 in clear cell renal cell carcinoma, with HIF-1α binding to the HRE on its promoter (Grampp et al., 2016). To date, whether expression of PVT1 is affected by hypoxia or HIF-1α in PC remains unclear. Here, we demonstrate positive feedback regulation among the lncRNA PVT1 and HIF-1α in PC cells at transcriptional and post-transcriptional levels. Our study also provides insights into the mechanisms of PVT1 and HIF-1α interactions.

Results

PVT1 and HIF-1α genetic profiles in human PC are associated with poor prognosis

Data concerning PVT1/HIF-1α expression and clinical information relevant to PC were downloaded from The Cancer Genome Atlas (TCGA) to investigate expression and clinical significance of PVT1/HIF-1α in PC. We confirmed the association of PVT1/HIF-1α expression with clinicopathological features of the illness by analyzing one independent cohort with 186 PC patients from TCGA in the cBioPortal (Figure 1). The following PVT1 genetic profiles were found: shallow deletions ($n = 6$), diploid ($n = 107$), gain-of-function ($n = 50$), and amplification ($n = 21$). The amplification logically led to the highest mRNA expression; however, no missense mutations and in-frame mutations were found. The following HIF-1α genetic profiles were

found: shallow deletions ($n = 15$), diploid ($n = 141$), and gain-of-function ($n = 28$). Missense mutations were found once. No in-frame mutations were found (Figure 1A).

We also performed stratified analyses of pancreas adenocarcinoma patient data from the independent cohort with cBioPortal on the provisional TCGA datasets. Overall survival (OS) analysis and DFS analysis revealed prognoses of patient groups with and without PVT1/HIF-1α gene amplification. Compared with patients without PVT1 gene amplification, those with PVT1 gene amplification had a decreased DFS ($P = 0.0011$) but not changed OS ($P = 0.0945$, Figure 1C). Median OS was 15.34 months in patients with PVT1 gene amplification whereas 20.6 months in patients without PVT1 gene amplification; median DFS was 7.56 months in patients with PVT1 gene amplification whereas 17.81 months in patients without PVT1 gene amplification (Figure 1B). HIF-1α gene amplification alone, however, was associated with a non-significant change in both OS ($P = 0.615$) and DFS ($P = 0.293$, Figure 1C). Median OS was 19.45 months in patients with HIF-1α gene amplification whereas 20.17 months in patients without HIF-1α gene amplification (Figure 1B). Interestingly, combined PVT1 and HIF-1α gene amplifications revealed better prognostic values than either PVT1 or HIF-1α gene amplification alone. Amplifications in both PVT1 and HIF-1α genes resulted in significantly poorer OS ($P = 0.0385$) and DFS ($P = 9.059E-04$, Figure 1C) among PC patients; median OS was 16.36 months in patients with gene amplifications of PVT1/HIF-1α whereas 21.42 months in those without PVT1 or HIF-1α gene amplifications (Figure 1B).

In addition, PC tissue chip from patient samples were collected and detected, in which 88 patient samples were available for the survival analysis. By fluorescence *in situ* hybridization (FISH) and immunohistochemistry (IHC) analyses in PC tumor tissues compared with para-cancerous tissues (Figure 2A and B; Supplementary Figure S1), we found that the expression levels of PVT1 RNA and HIF-1α protein were both significantly increased in cancer tissues compared with para-cancerous tissues (both $P < 0.01$, Figure 2C). Associations between the expression levels of PVT1 RNA and HIF-1α protein were assessed and the result suggested that the expression of PVT1 RNA was positively correlated with the expression of HIF-1α protein (the Pearson correlation coefficient $r = 0.7488$, $P < 0.01$, Supplementary Figure S2). OS analysis was also performed to reveal prognoses of patient groups with high or low level of PVT1/HIF-1α. Consistent with the results from TCGA, Kaplan−Meier survival analysis showed that the prognosis of PC patients with high PVT1 and HIF-1α expression was worse than that of PC patients with low PVT1 or HIF-1α expression. Compared with patients with low expression of both PVT1 and HIF-1α, or the two status of intermediate (PVT1 high/HIF-1α low and PVT1 low/HIF-1α high), those with high PVT1 and HIF-1α expression in combination had a significantly decreased OS (Figure 2D and E). Univariate Cox analysis followed by multivariate Cox regression analysis identified that PVT1 and HIF-1α co-expression status was an independent prognostic factor for OS of patients with PC (Supplementary Table S2).
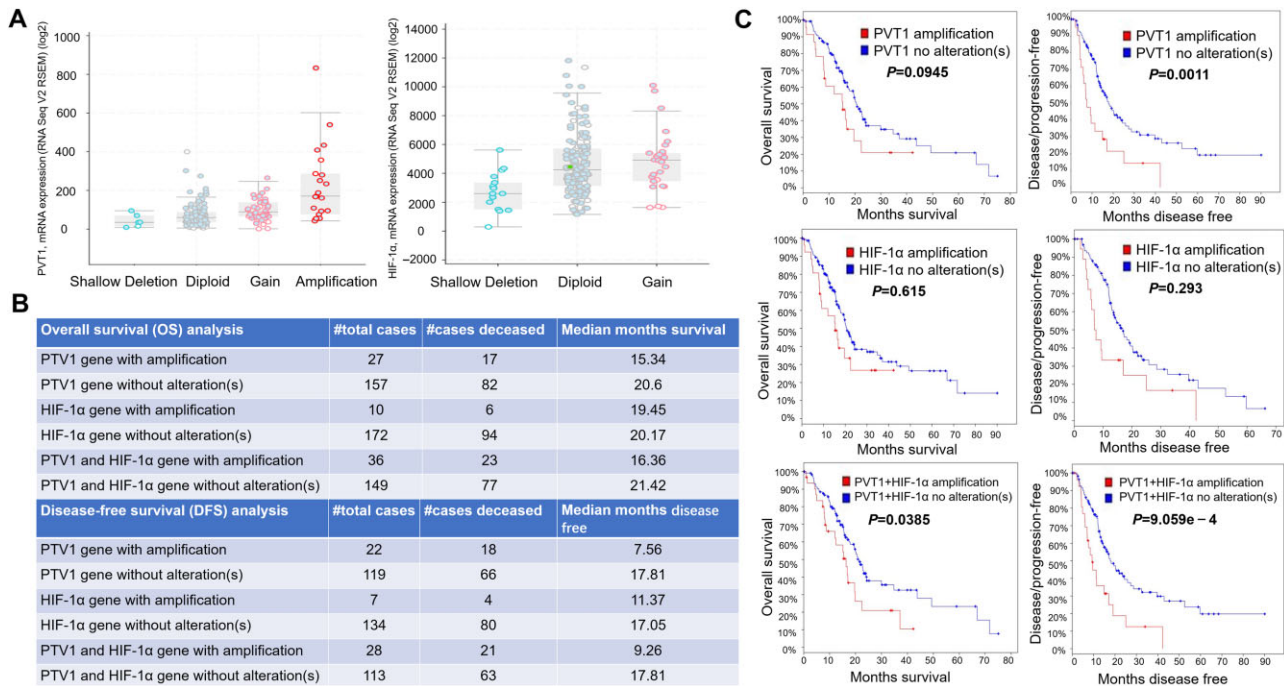
Figure 1 PVT1 and HIF-1α are associated with poor prognosis in PC from TCGA. (**A**) Analysis of genetic alterations of PVT1 and HIF-1α by cBioPortal in 186 PC patients using cBioportal. Shallow deletion, heterozygously deleted; diploid, two alleles present; gain, low-level gene amplification event; amplification, high-level gene amplification event. (**B**) PVT1 and HIF-1α gene amplifications associate with cases and median survival months of OS and DFS in PC patients. (**C**) Kaplan–Meier survival curves show poor OS and DFS with PVT1 and HIF-1α gene amplifications in combination when compared with the PVT1 or HIF-1α gene amplifications alone.

PVT1 and HIF-1α reciprocally regulate the expression of one another and form a positive feedback loop

Hypoxia is a hallmark of solid tumors, including PC, and is associated with metastases, therapeutic resistance, and poor patient survival. Interestingly, we found that PVT1 expression was induced by hypoxia in PC. Results revealed that PVT1 expression was significantly induced by hypoxia in all three cell lines ($P < 0.01$, Figure 3A). To investigate the impact of silencing PVT1 and HIF-1α on each other, two respective siRNAs against PVT1 and HIF-1α were used to perform the basic experiments. The quantitative real-time polymerase chain reaction (qRT-PCR) results indicated that both siPVT1-1 and siPVT1-2 effectively knocked down PVT1; meanwhile, both siHIF-1α-1 and siHIF-1α-2 effectively knocked down HIF-1α. If not specified, siPVT1-1 and siHIF-1α-1 would be used in the following molecular-level experiments (Supplementary Figure S3). Lower HIF-1α mRNA levels were found in both siPVT1-1 and siPVT1-2 groups compared with controls. Lower PVT1 levels were found in both siHIF-1α-1 and siHIF-1α-2 groups compared with controls. Increased HIF-1α mRNA levels were found in the PVT1 overexpression group compared with that in controls. Overexpression of HIF-1α by adenovirus infection upregulated PVT1 levels ($P < 0.01$, Figure 3B). Meanwhile, HIF-1α expression was greatly attenuated by PVT1 siRNAs under normoxic condition but not under hypoxic condition ($P < 0.05$, Figure 3C). The PVT1 siRNA knockdown efficiencies under both normoxic and hypoxic conditions in all three cell lines were

tested and compared, and the results showed that knockdown of PVT1 by two siRNAs could downregulated PVT1 expression under normoxic condition but not under hypoxia condition. Thus, PVT1 lost the ability to regulate HIF-1α under hypoxic condition (Figure 3D). These findings suggest that knockdown of PVT1 could attenuate HIF-1α upregulation only under normoxic condition.

We further explored the regulatory effects of PVT1 on HIF-1α protein expression in PANC-1 cell line by western blotting. We found that the levels of HIF-1α protein decreased after PVT1 knockdown under normoxic condition but not under hypoxic condition (Figure 3E), while PVT1 overexpression increased HIF-1α protein levels under both normoxic and hypoxic conditions (Figure 3F). Our findings suggest that PVT1 is a HIF-1α-responsive lncRNA and PVT1 regulates HIF-1α expression in the three PC cell lines under normoxic condition.

HIF-1α upregulates PVT1 transcription by binding to its promoter region and stabilizes PVT1 by binding to the transcript

Taking into consideration that HIF-1α is a potent transcription factor that fulfills its oncogenic functions by activating the transcription of downstream targets within tumor cells, we investigated whether PVT1 served as a direct transcriptional target of HIF-1α. Considering that PVT1 isoforms are variably expressed across human tissues, first, we tried to clarify which isoforms are expressed in PC cell lines and tumor tissues from
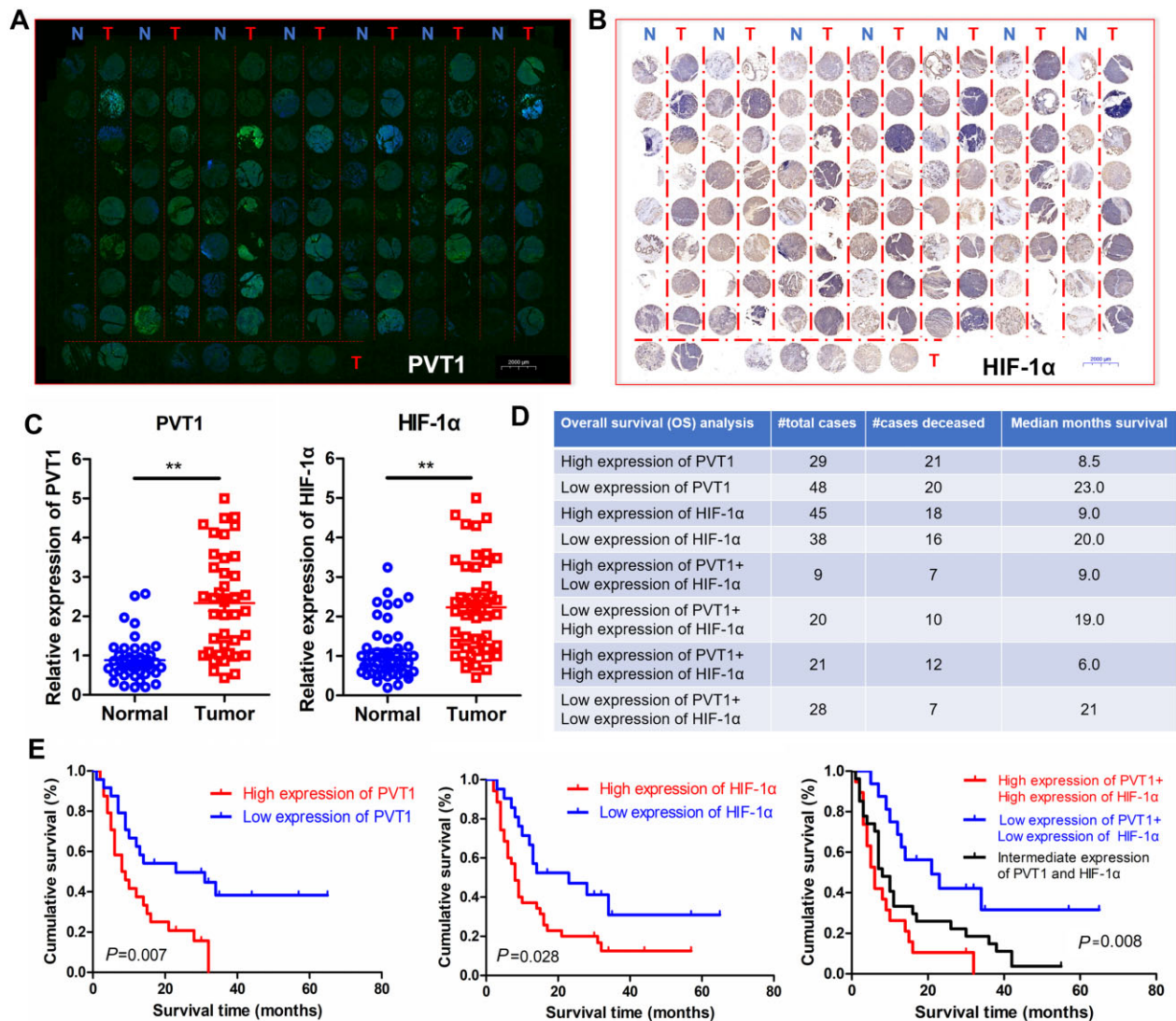
Figure 2 PVT1 and HIF-1α are associated with poor prognosis in PC patient samples. (**A** and **B**) FISH and IHC analysis of the expression levels of PVT1 and HIF-1α in the representative PC patient samples in cancer tissues compared with para-cancerous tissues. (**C**) The expression levels of PVT1 RNA and HIF-1α protein both significantly increase in cancer tissues compared with para-cancerous tissues. (**D**) PVT1 RNA and HIF-1α protein expression levels associate with cases and median survival months of OS in PC patients. (**E**) Kaplan–Meier survival curves show poor OS associated with high expression of PVT1 RNA and HIF-1α protein. The intermediate expression of PVT1 and HIF-1α refers to the high expression of PVT1 + low expression of HIF-1α or low expression of PVT1 + high expression of HIF-1α.

nude mice. The results suggested that the full-length transcript of PVT1 could be detected (Supplementary Figure S4). Then, the chromatin immunoprecipitation (ChIP) analysis was performed using antibodies against HIF-1α and digested chromatin from the extracts of PANC-1, Mia PaCa-2, and BxPC-3 cells. Purified DNA was analyzed by qRT-PCR (Figure 4A) and fragments of the PVT1 promoter were detected by semi-quantitative PCR (qPCR) (Figure 4B), verifying that HIF-1α binds to the PVT1 promoter region. Biotin RNA–protein pull-down assays evaluating whether HIF-1α binds to PVT1 revealed HIF-1α within the PVT1-bound complex in all three PC lines (Figure 4C). In addition, the PVT1-bound complex was confirmed by western blotting in all three lines.

Bioinformatically, we searched putative binding sites (i.e. HREs) for HIF-1α in the promoter region of PVT1. The online TFSEARCH (http://www.cbrc.jp/research/db/TFSEARCH.html) database was used. As shown in Figure 4D, we found four putative HREs (5′-RCGTG-3′) within 2000 bp upstream of the transcriptional start of PVT1. Dual-luciferase reporter assays were used to explore whether HREs within the PVT1 promoter confer HIF-1α-dependent transcriptional activity. A pGL4-PVT1-promotor plasmid was constructed by inserting DNA fragments of the PVT1 promoter into a Renilla luciferase plasmid. Findings of these assays indicated that knockdown of HIF-1α reduced PVT1 promoter activity whereas overexpression of HIF-1α
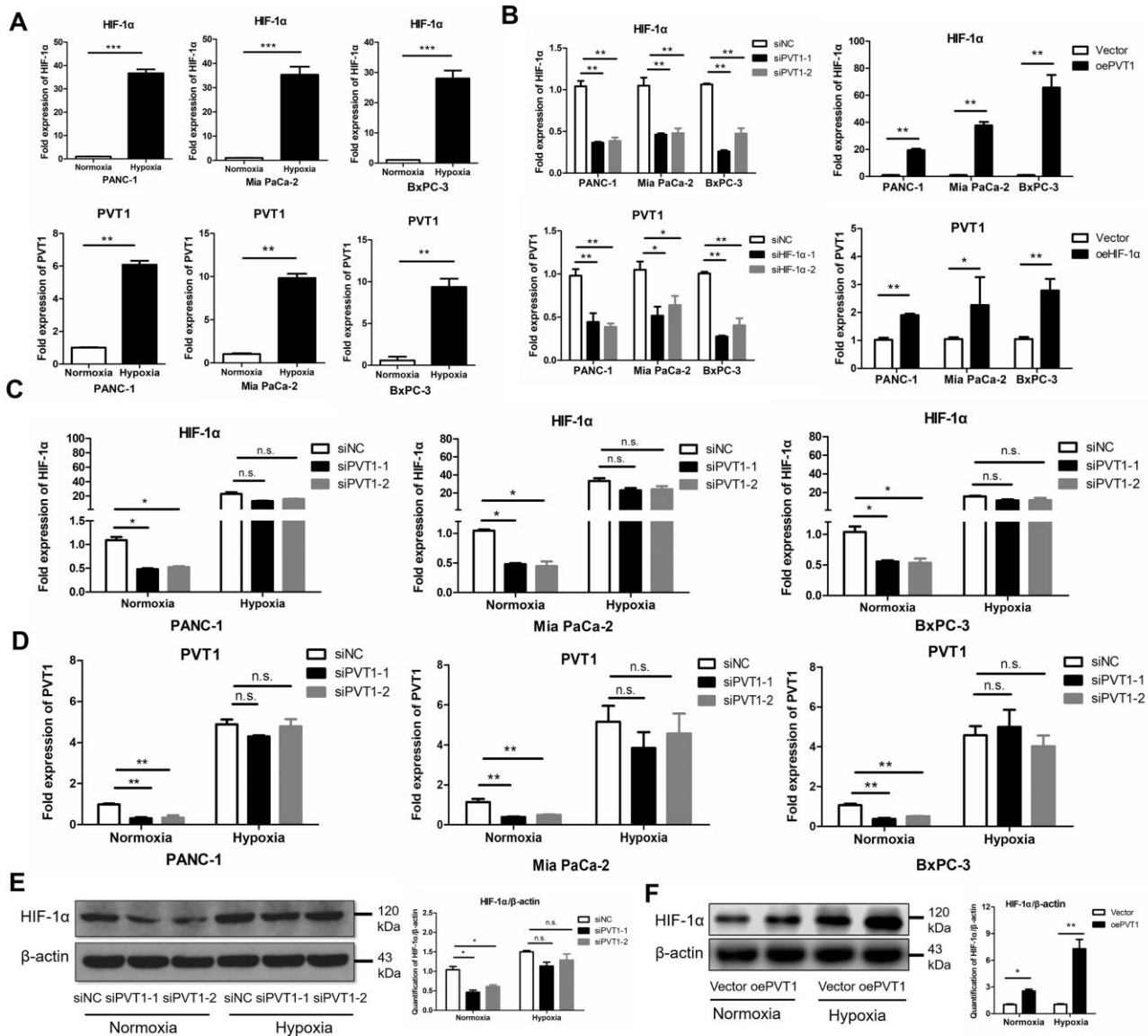
Figure 3 The feedforward regulatory loop between PVT1 and HIF-1α in PC cell lines. (**A**) Increased HIF-1α and PVT1 expression was induced by hypoxia in PANC-1, Mia PaCa-2, and BxPC-3 cell lines. *$P < 0.05$, **$P < 0.01$. (**B**) Lower HIF-1α mRNA levels were found in the PVT1 siRNA groups compared with controls. Lower PVT1 levels were found in the HIF-1α siRNA groups compared with controls. Overexpression of PVT1 by adenovirus infection upregulated HIF-1α mRNA levels, and overexpression of HIF-1α by adenovirus infection upregulated PVT1 levels. *$P < 0.05$. (**C**) HIF-1α mRNA levels after PVT1 knockdown under both normoxic and hypoxic conditions were tested in all three PC cell lines. *$P < 0.05$, **$P < 0.01$. (**D**) The PVT1 siRNA knockdown efficiencies under both normoxic and hypoxic conditions in all three cell lines were tested and compared. **$P < 0.01$. (**E**) HIF-1α protein levels after PVT1 knockdown under normoxic and hypoxic conditions in PANC1 cell line were detected by western blotting. *$P < 0.05$. (**F**) HIF-1α protein levels after PVT1 overexpression under both normoxic and hypoxic conditions in PANC1 cell line were detected by western blotting. *$P < 0.05$, **$P < 0.01$.

stimulated PVT1 promoter activity in 293T cells (Figure 4E), suggesting that HIF-1α binds to HREs of the PVT1 promoter to activate its transcription.

Despite progress in functional characterization, little is known concerning post-transcriptional regulation of lncRNAs and their half-lives. To examine the stability of PVT1, we blocked *de novo* synthesis of RNA with actinomycin D in HIF-1α siRNA-treated cells and measured remaining transcripts of the lncRNA PVT1, relative to a control gene, using qRT-PCR at several time points. We found that the decay rate of PVT1 was more rapid in HIF-1α knockdown cells than in control cells (Figure 4F). The above results suggested that expression of HIF-1α was required for efficient transcription and stabilization of the lncRNA PVT1.
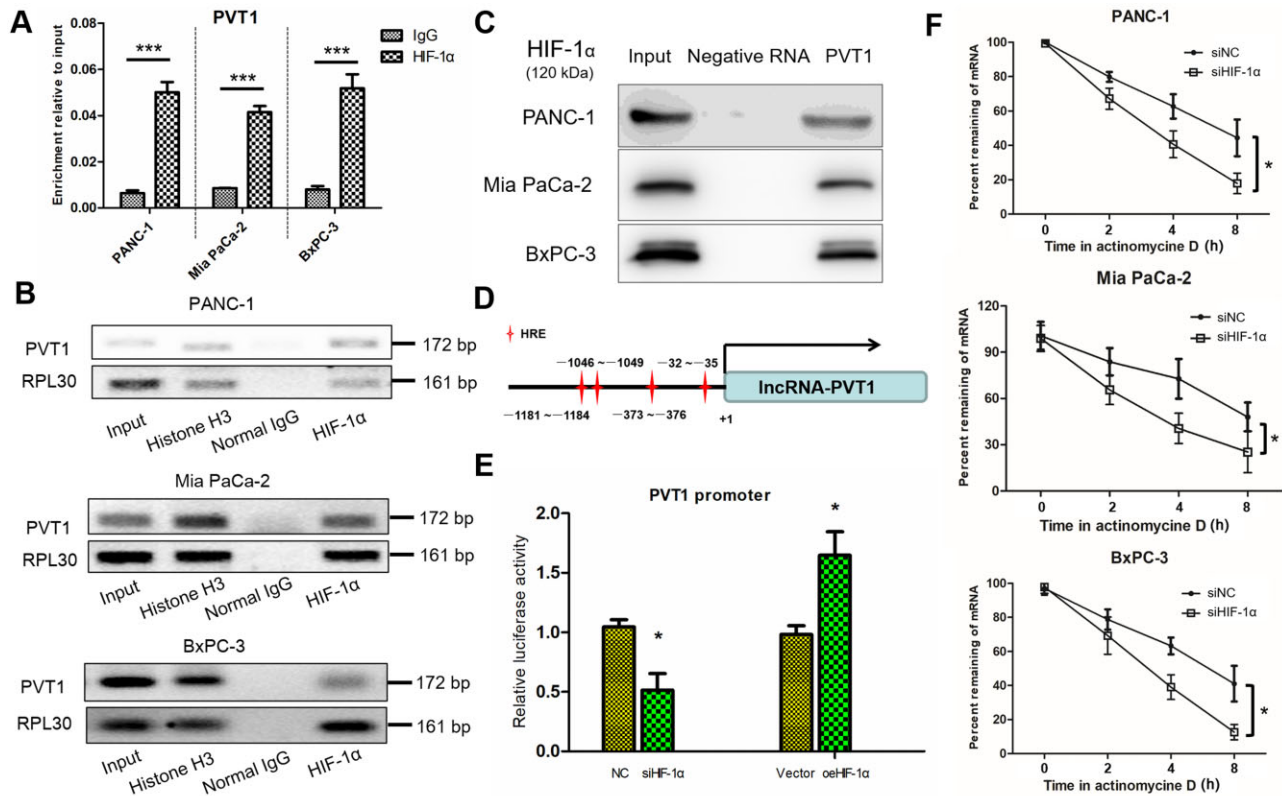
Figure 4 PVT1 interacts with HIF-1α in PC cells. (**A**) ChIP assays were performed using digested chromatin from PC cells and the indicated ChIP-validated HIF-1α antibodies. Purified DNA was analyzed by qRT-PCR using exon primers. ***$P < 0.001$, compared with the IgG group. (**B**) The fragments of the PVT1 promoter were detected in HIF-1α-immunoprecipitated chromatin from the ChIP analysis of all three PC lines by qPCR. (**C**) HIF-1α protein was detected by western blotting using the corresponding antibody in biotin-RNA pull-down assays among all three PC cell lines. (**D**) Model graph proposing four putative HREs within 2000 bp upstream of the transcriptional start of PVT1. (**E**) Dual-luciferase reporter assays reveal binding of HIF-1α to PVT1 promoter HREs to activate its transcription in 293T cells. *$P < 0.05$, compared with the pGL4-basic group. (**F**) PC cells transfected with HIF-1α siRNA were treated with actinomycin D (2.5 µg/ml) to block *de novo* transcription. PVT1 mRNA levels were assessed by qRT-PCR analysis and normalized to GAPDH levels at indicated time points. The percentage of mRNA that remained was plotted. Error bars show SDs.

HIF-1α is a direct transcriptional target of PVT1

We subsequently aimed to elucidate the genomic binding sites of PVT1 and their relationship with HIF-1α occupancy via chromatin isolation by RNA purification (ChIRP) assay. PANC-1 cells were cross-linked and sonicated, and their chromatin complexes were hybridized with two different pools of biotinylated probes ('PVT1-even' and 'PVT1-odd' probe sets). RNA–protein–DNA complexes were immunoprecipitated with magnetic streptavidin beads. After a series of washes, isolated complexes were treated with RNase H and RNase A to remove RNA components, resulting in RNA-binding proteins and genomic DNA. ChIRP analysis revealed that PVT1 interacts with the HIF-1α promoter in PC cells *in vitro*. Both pools of tiling oligonucleotides co-precipitated target promoters of HIF-1α (Figure 5A).

Dual-luciferase reporter assays were performed to explore whether the binding of PVT1 to the HIF-1α promoter activates the transcription of HIF-1α. A 2000-bp-long pGL4-HIF-1α-promotor plasmid was constructed for this experiment as shown in Figure 5B. We found that overexpression of PVT1 stimulated HIF-1α promoter activity, which was reduced by PVT1 knockdown in 293T cells (Figure 5B). The stability of HIF-1α mRNA, as measured by detection of mRNA degradation after actinomycin D treatment, was found unaltered after PVT1 knockdown, indicating that reduced stability of HIF-1α was not responsible for lower levels of HIF-1α mRNA in PVT1 siRNA-treated cells (Figure 5C). These data suggest that PVT1 likely serves as a transcriptional regulator of HIF-1α in PC cells and that PVT1-specific response elements (PVT1-RE) within the HIF-1α promoter play vital roles in a positive feedback loop.

Hypoxia-induced PVT1 stabilizes HIF-1α protein level

Previous studies have reported that normoxia-induced HIF-1α SUMOylation promotes HIF-1α degradation via a VHL and proteasome-dependent mechanism (Du et al., 2019). To explore whether PVT1 regulates HIF-1α stability by interacting with HIF-1α protein, PANC-1 cells were cultured under hypoxic (1% O_2), normoxic (20% O_2), and/or MG132 (5 µM) conditions
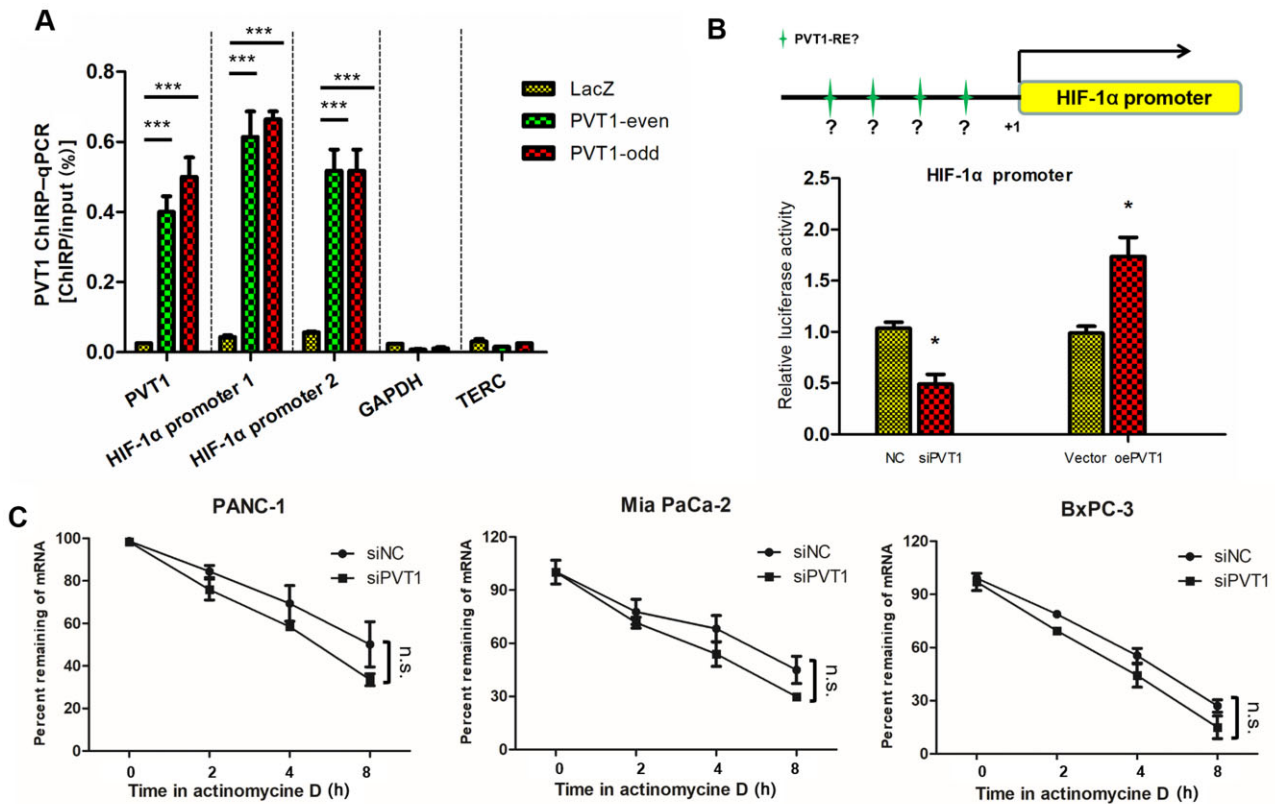
Figure 5 HIF-1α is a direct transcriptional target of PVT1. (**A**) Chromatin was cross-linked to RNA–protein–DNA complexes. Biotinylated probes were hybridized to PVT1, while chromatin complexes were purified using magnetic streptavidin beads and washed thoroughly. LncRNA-bound DNA was eluted with a cocktail of RNase A and RNase H. Antisense DNA tiling probes were grouped into 'even' and 'odd' sets based on their RNA positions. ChIRP assays reveal that PVT1 occupies two HIF-1α promoter regions in PC cell lines. (**B**) Dual-luciferase reporter assays reveal that PVT1 binds to putative HIF-1α promoter sites to activate its transcription in 293T cells. *$P < 0.05$, compared with the pGL4-basic group. (**C**) HIF-1α transcript decay curves after blocking transcription in PC cells with actinomycin D and measuring transcript remaining relative to a control gene using qRT-PCR in PVT1 knockdown cells. Error bars show SDs.

for 24 h. In both PVT1 knockdown and control cells, HIF-1α protein levels were analyzed by western blotting. The results indicated that such HIF-1α decrease due to PVT1 knockdown was corrected by treatment with the proteasome inhibitor MG132 (Figure 6A). Time course assays using PANC-1 cells transfected with either control or PVT1 siRNA and treated with cycloheximide (CHX) (20 μg/ml) under either normoxia or hypoxia with subsequent determination of HIF-1α protein expression by western blotting indicated that PVT1 knockdown led to a decrease in HIF-1α half-life under hypoxic condition (Figure 6B and C). Such findings suggest that PVT1 interacts with HIF-1α protein and that hypoxia-induced PVT1 protects HIF-1α protein from proteasome-dependent degradation.

Knockdown of PVT1 inhibits HIF-1α-induced cell proliferation, migration, and invasion

To further determine whether the functional roles of HIF-1α in hypoxia were dependent on the activity of PVT1, we investigated whether knockdown of PVT1 by siRNA could rescue PC tumorigenesis and metastasis induced by HIF-1α overexpression. Eight hours after infection with recombinant adenovirus encoding HIF-1α or vector adenovirus, the HIF-1α-upregulated PANC-1 cells were transfected with PVT1 siRNA (oeHIF-1α+siPVT1) and subjected to a rescue study. Cell viability/proliferation assay showed that the absorbance in the oeHIF-1α+siPVT1 group was less than that in the HIF-1α overexpression group (Figure 7A). Cell clonogenicity assay demonstrated that PVT1 siRNA significantly inhibited the clone formation in PANC-1 cells with HIF-1α adenoviral infection (Figure 7B and C). Strikingly, transwell assay demonstrated that the numbers of migrated and invaded cells after PVT1 siRNA transfection were both reduced compared with HIF-1α overexpression individually (Figure 7D and E). Furthermore, in the wound-healing assay performed with PANC-1 cell line, we found that HIF-1α-overexpressing cells were more proficient than vector adenovirus-transduced cells at closing an artificial wound created over a confluent monolayer in 24 h, which was reverted by PVT1 depletion in partial (Figure 7F and G). To show the influence of PVT1 and HIF-1α on the proliferation and metastasis *in vivo*, a tumor-bearing animal model was used.
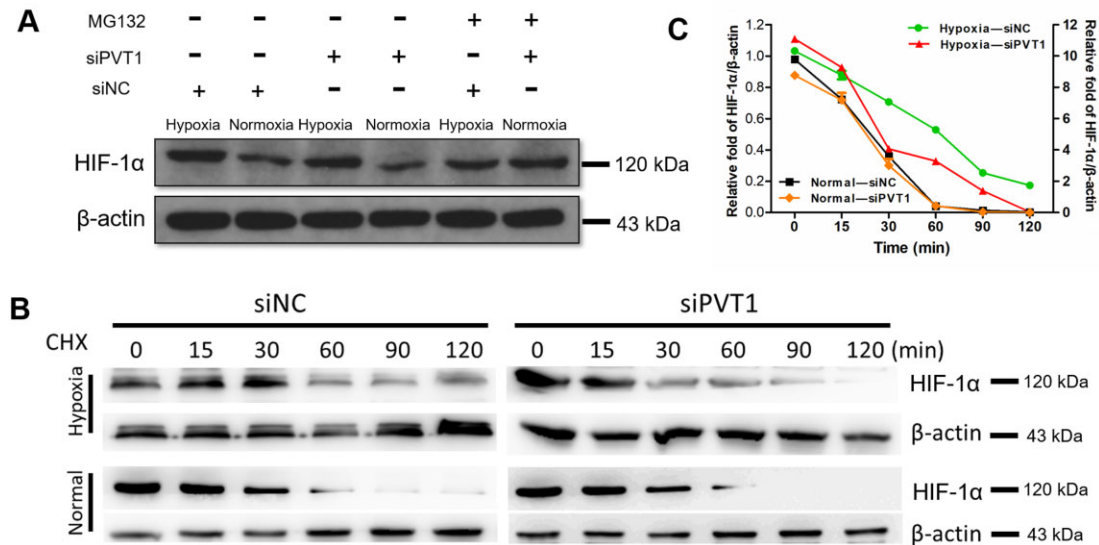
Figure 6 Hypoxia-induced PVT1 stabilizes HIF-1α protein levels. (**A**) PC cells expressing either control or PVT1 siRNA were cultured under normoxic or hypoxic condition in the presence or absence of MG132 (5 μM) for 24 h. Cell lysates were then analyzed by western blotting. (**B**) PC cells expressing either control or PVT1 siRNA were cultured under normoxic or hypoxic condition for 24 h before being treated with CHX (20 μg/ml) for indicated periods of time. Cell lysates were analyzed by western blotting. (**C**) Quantification of HIF-1α protein expression in **B**.

HIF-1α overexpression, HIF-1α overexpression with PVT1 knock-down, or control PANC-1 cells were subcutaneously injected into nude mice, and then the tumor growth was evaluated. The results demonstrated that cells lacking PVT1 suppressed HIF-1α-enhanced PC tumorigenesis (Figure 7H and I).

Discussion

Human solid tumors generally thrive under hypoxic conditions and such states have been reported to associate with oncogenesis, metastasis, disease recurrence, and therapeutic resistance (Huang, 2013; Yuen and Díaz, 2014; Erickson et al., 2015; Chen et al., 2016). Studies concerning cell responses to hypoxia within tumors are of importance in understanding cancer progression and are helpful in uncovering novel diagnostic and therapeutic approaches toward successful disease management. A specific group of lncRNAs have been defined as 'hypoxia-responsive' in cancer settings, either upregulated or downregulated by hypoxia, indicating that these non-coding genomes are involved in adaptation to hypoxia by malignant cells (Choudhry et al., 2016; Shih et al., 2017; Shih and Kung, 2017; Kapinova et al., 2018).

The lncRNA PVT1, located adjacent to the MYC locus on 8q24, has been reported to be overexpressed in a variety of human malignancies (Grampp et al., 2016). In PC, PVT1 overexpression has been confirmed to correlate with poor patient prognosis (You et al., 2011; Colombo et al., 2015). Recent studies revealed that hypoxia upregulates PVT1 in a variety of cancers, suggesting that its expression is influenced by hypoxic conditions (Cui et al., 2016; Shih and Kung, 2017). We confirmed that PVT1 was upregulated under hypoxia in all three PC

cell lines and that such upregulation was HIF-1α dependent. We also demonstrated that the expression of HIF-1α in PC was, in turn, modulated by PVT1, and thus constituted a positive feedback loop (i.e. the reciprocal regulation of PVT1 and HIF-1α).

In this study, we aimed to elucidate the underlying mechanism by which the lncRNA PVT1 was upregulated during hypoxia in PC. Previously, PVT1 was reported to be transcriptionally activated by HIF-1α through the binding of this protein with its promoter in renal clear cell carcinoma (Grampp et al., 2016). As a transcription factor, HIF-1α has been known to carry out its functions by binding to the promoter of downstream effector genes and stimulating their transcriptional activities. We verified, by ChIP analysis and biotinylated RNA–protein pull-down assays, that the PVT1 promoter, harboring four putative HREs, is a direct binding target for HIF-1α in PC. We subsequently confirmed transcriptional upregulation by dual-luciferase reporter assays.

RNA stability is another important factor that plays a role in the regulation of lncRNA expression (Wang et al., 2014). To date, there have been no reports implicating any correlations between HIF-1α and the stability of the lncRNA PVT1. We demonstrated that HIF-1α prolongs PVT1 half-life by binding to it. Our data thus reveal that, in response to hypoxia, PVT1 is transcriptionally upregulated and post-transcriptionally stabilized by HIF-1α in PC cells.

Hypoxia-responsive lncRNAs have also been reported to modulate HIF-1α expression via various mechanisms. Most of these modulations seem to work indirectly (Shih and Kung, 2017). For instance, in PC, the lncRNA ENST00000480739 was identified to suppress HIF-1α expression by increasing osteosarcoma amplified-9 (OS-9) transcription, on account of OS-9
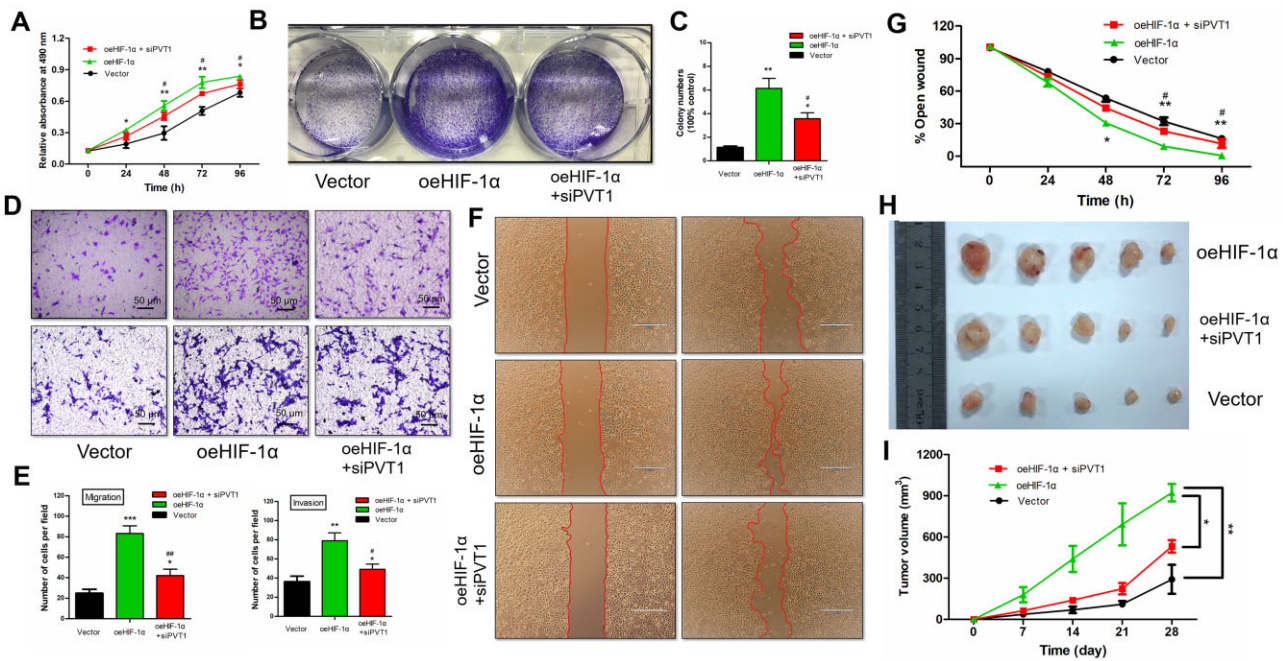
Figure 7 Knockdown of PVT1 inhibits HIF-1α-induced tumorigenesis and metastasis. (**A**) PANC-1 cells were infected with oeHIF-1α adenovirus or vector adenovirus and then transfected with PVT1 siRNA in oeHIF-1α group. The cell viability of the transfected PANC-1 cells was measured by MTS at 0, 24, 48, 72, and 96 h after transfection. *$P < 0.05$, **$P < 0.01$, compared with vector group; #$P < 0.05$, compared with oeHIF-1α group. (**B** and **C**) Representative images of cell clonogenicity assay and normalized cell clone formation data in PANC-1 cells. *$P < 0.05$, **$P < 0.01$, compared with vector group; #$P < 0.05$, compared with oeHIF-1α group. (**D** and **E**) Representative images of cell migration and invasion assays in PANC-1 cells. Graphs indicate the average number of cells per field of the indicated cell lines in migration and invasion assays. Magnification, ×100. *$P < 0.05$, **$P < 0.01$, ***$P < 0.001$, compared with vector group; #$P < 0.05$, ##$P < 0.01$, compared with oeHIF-1α group. (**F**) Wound-healing assays in PANC-1 cells were performed after infection with oeHIF-1α adenovirus or vector adenovirus and then transfection with PVT1 siRNA in oeHIF-1α group. Pictures were taken at 0 and 24 h after artificial wound was created. (**G**) Quantification of the wound-healing assay results. (**H**) Nude mice were subcutaneously injected with 5×10^6 treated PANC-1 stable cells, and then tumor growth was evaluated. (**I**) Tumors were dissected and photographed after 5 weeks. Tumor volumes were calculated. Data represent mean ± SD ($n = 5$).

being an HIF-1α binding protein and mediating its degradation (Sun et al., 2014). Likewise, the lncRNA RERT was reported to downregulate HIF-1α through activation of EGLN2 transcription (Zhu et al., 2012). In several human malignancies, including hepatocellular carcinoma, colorectal carcinoma, gallbladder cancer, and squamous lung cancer, the lncRNA-LET is downregulated. This leads to increased NF90 activity, which subsequently increases the stability of HIF-1α mRNA (Yang et al., 2013). The lncRNA PVT1 was reported to work as a competing endogenous RNA in gastric cancer, interacting with miR-186 and leading to the reversion of miR-186-inhibited mediation of HIF-1α inhibition (Huang et al., 2017). Moreover, PVT1 was reporter to suppress the transcription of miR-18b-5p through DNA methylation and thus regulate its downstream target gene HIF-1α in gallbladder cancer (Jin et al., 2020) However, our study found that PVT1 upregulates HIF-1α transcription by binding to its promoter.

In previous studies, lncRNAs have been reported to exhibit sequence-specific binding properties. Their binding to other nucleic acids through one-to-one base pair interactions thus influence the activity and metabolism of target DNA or RNA (Chu et al., 2011). Some lncRNAs regulate transcription of target genes by recruiting transcription factors to their target gene promoters, thereby activating gene expression (Feng et al., 2006). However, the precise mechanism by which PVT1 upregulates the transcription of HIF-1α after binding to its promoter remains elusive and should be studied in further detail.

In this study, we also analyzed the effect of PVT1 overexpression on post-transcriptional regulation of HIF-1α in PC cells. Using biotinylated RNA–protein pull-down and protein degradation assays, we demonstrated that the PVT1 transcript binds to HIF-1α protein and reduces its degradation. Xu et al. (2017) reported that PVT1 increased FOXM1 protein stability by inhibiting its 26S proteasome-mediated degradation in the setting of gastric cancer. Our findings revealed that PVT1-mediated regulation of HIF-1α expression plays vital roles, in both transcriptional and post-transcriptional stages. Interestingly, lncRNA–protein interactions between PVT1 and HIF-1α were found to lead to increased PVT1 stability in this study. This paper thus demonstrates a reciprocal regulation between PVT1 and HIF-1α, which can essentially be described as a positive feedback loop (Figure 8). Thus, we hypothesized that the functional roles of

HIF-1α-enhanced PC tumorigenesis and metastasis in hypoxia were dependent on the activity of PVT1.

As a core regulator of tumor cell adaptation to hypoxia, HIF-1α is primarily activated in hypoxic environments. Cellular levels of HIF-1α have, however, been reported to be elevated under certain circumstances due to genetic and signaling pathway alterations, even under normoxic conditions (Hansen et al., 2011). Overexpression of HIF-1α has been considered related to chemo-resistance in PC (Peng et al., 2016). Based on our work, the PVT1/HIF-1α feedback loop can be presupposed to amplify hypoxia-induced expression of HIF-1α and lead to maintenance of high HIF-1α expression in PC cells, even when hypoxic stimuli abate. Overexpression of PVT1 can increase HIF-1α mRNA and protein expression under normoxia. The continuous activation of the PVT1/HIF-1α feedback loop likely promotes PC pathogenesis. In our study, PC patients with both highly expressed PVT1 and HIF-1α exhibited worse survival rates than patients overexpressing only one of these markers. Such findings emphasize the prognostic value of the PVT1/HIF-1α feedback loop in predicting PC patient outcomes and highlight the importance of this loop in the progression of PC. Targeting the PVT1/HIF-1α loop may be a novel therapeutic strategy for PC treatment in the near future.

Materials and methods
Cell lines and cell culture
PANC-1 (human PC cell line) and BxPC-3 (human pancreatic adenocarcinoma cell line) cells were obtained from the American Type Culture Collection (ATCC). Mia PaCa-2 (human PC cell line) cells were purchased from the China Center for Type Culture Collection (CCTCC). PANC-1 and Mia PaCa-2 cells

Figure 8 A schematic diagram shows the positive feedback loop of PVT1 and HIF-1α in PC. Our study identified the reciprocal link between PVT1 and HIF-1α, reflecting the underlying molecular mechanism of their biological interactions. PVT1 binds to the HIF-1α promoter and activates its transcription. Meanwhile, PVT1 binds to HIF-1α and increases HIF-1α post-translationally. Moreover, PVT1 is also an HIF-1α-responsive lncRNA and binds to the PVT1 promoter to activate its transcription. The positive feedback loop among PVT1 and HIF-1α promotes PC pathogenesis and appears to be a promising target for PC therapy.

were cultured in Dulbecco's modified Eagle's medium containing 10% fetal bovine serum (FBS), while BxPC-3 cells were cultured in 1640 medium containing 10% FBS. Cells were maintained under either normoxic (37°C, 5% CO_2, 20% O_2) or hypoxic (37°C, 5% CO_2, 1% O_2) condition.

Recombinant adenovirus packaging and siRNA synthesis
Recombinant adenoviruses carrying PVT1/HIF-1α-pcDNA3.1(oePVT1/oeHIF-1α) and GFP-pcDNA3.1 vector (vector) were packaged by Shanghai GeneChem Co., Ltd. PVT1/HIF-1α siRNAs were synthesized by Shanghai GenePharma Company and transfected into the PC cell lines using Lipofectamine RNAiMax (Invitrogen) according to the manufacturer's instructions. siRNAs targeting PVT1 including siPVT1-1: 5′-CCUGCA UAACUAUCUGCUUUT-3′ and siPVT1-2: 5′-CCCAACAGGAGGACAG CUUTT-3′, siRNAs targeting HIF-1α including siHIF-1α-1: 5′-CCG CUGGAGACACAAUCAUAU-3′ and siHIF-1α-2: 5′-CCAGTTATGAT TGTGAAGTTA-3′, and a scrambled control siRNA (NC siRNA) were synthesized. Approximately 2×10^5 cells were plated per 25-cm^2 flask at least 24 h before transfection to achieve 50%–70% confluency and then transfected with either 60 nM PVT1/HIF-1α siRNAs or NC siRNA.

Extraction of TCGA data
TCGA data of PVT1/HIF-1α expression in PC patients and noncancerous tissues were downloaded to analyze PVT1/HIF-1α expression in these patients as well as correlations with PC clinical parameters. The analyses for PC, named 'Pancreatic Adenocarcinoma (TCGA, Provisional)', are available on cBioPortal with 186 samples. Data concerning PVT1/HIF-1α gene amplifications were available at cBioPortal OncoPrint (http://www.cBioPortal.org/index.do) (Gao et al., 2013) and were analyzed to evaluate the status of PVT1 and HIF-1α genes in the development of PC. For the analysis, RNA sequencing data from TCGA were used (RNA Seq V2 RSEM) with two standard deviations (SDs) from the mean and a threshold of ±2.0. The mRNA z-scores were precomputed from the expression values and compared with the expression distribution of each gene associated with the tumors that are diploid for this gene, and a P-value <0.05 was set as the cutoff criterion. Kaplan–Meier survival curves were drawn to examine the impact of PVT1/HIF-1α amplifications on the prognosis of PC patients.

Patients and tissue samples
PC and adjacent tissue sections from PC tissue chip were collected retrospectively from archival material stored in the biobank center in the National Engineering Center for Biochip at Shanghai. Samples included a total of 150 patients who had undergone a resection surgery between September 2004 and December 2008. Written informed consent for the tissue specimens was received from each participant, and the study was
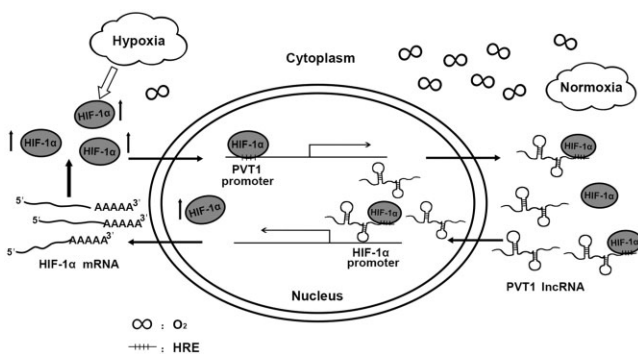
approved by the ethical committee of the biobank center-related hospitals. At the time of the last follow-up in December 2011, 88 patient samples were available for the survival analysis. A case processing summary of clinical and pathological data of these 88 patients was provided in Supplementary Table S1 and Figure S1. The tissue sections were deparaffinized, repaired with citrate antigen, blocked, and then incubated with the HIF-1α antibody (Cell Signaling Technology, 1:200) at 4°C overnight in incubator. Tissue sections were stained with DAB and again stained with hematoxylin. Images were captured using a photomicroscope and analyzed. The hybridization was performed overnight with PVT1 probes. Specimens were analyzed on a Nikon inverted fluorescence microscope. The PVT1 probe for FISH was 5′-CTGTAATACCAGCTACTCGG-3′. Patients were divided into low- and high-expression groups using the median values of PVT1/HIF-1α expression as the cutoff values according the histochemistry score of FISH/IHC analysis.

ChIP

ChIP analysis was carried out as described previously (Kim and Dekker, 2018). Briefly, HIF-1α protein was immunoprecipitated with ChIP-grade HIF-1α monoclonal antibodies. A no-antibody control was also included to confirm immunoprecipitation specificity. ChIP-enriched DNA was isolated with the Qiaquick PCR Purification Kit (Qiagen). Subsequent qPCR fractionation of ChIP-enriched DNA and 100 nM primers in a total volume of 20 μl was conducted to assess the amount of precipitated DNA. Purified DNA was analyzed by qRT-PCR using exon primers, according to the manufacturer's instructions (Cell Signaling Technology). Standard curves were drawn according to 0.1–100 ng of sonicated genomic DNA amplified by qPCR as a reference. The following PVT1 primers were used for qPCR: F1: 5′-TGAGTAACCCCCACCCCATT-3′; R1: 5′-CCGAACCTGAGATGA TCCAC-3′; F2: 5′-GTGGATCATCTCAGGTTCGG-3′; R2: 5′-TCAAGC GATTCTCCTGCCTC-3′ (Supplementary Table S5).

Biotin pull-down assay

The PVT1 plasmid was linearly cut, transcribed and biotin-labelled *in vitro* with Bio-16-UTP (Life Technologies) using a MAXIscript® T7 Transcription Kit (Life Technologies), treated with RNase-free DNase I (Promega), and purified with RNeasy Mini Kit (QIAGEN). Protein–RNA interactions were enriched using a Pierce Magnetic RNA–Protein Pull-Down Kit (Life Technologies) for the lysates of the three PC cell lines. The biotin-RNA pull-down assay was carried out by incubating 1.5 μg of biotinylated RNA antisense transcripts with 250 μg of cytoplasmic lysate prepared with Buffer A for 30 min at room temperature. Then, 100 μl of Streptavidin MagneSphere paramagnetic particles (Promega) were saturated with 150 μg tRNA and added to the extract for 15 min at room temperature. After washing with EMSA buffer for three times, bound RNA and protein complexes were eluted and subsequently analyzed by qRT-PCR and western blotting, respectively. Biotinylated transcripts were obtained from PCR-generated templates using the MAXIscript *in vitro* transcription system (Life Technologies).

ChIRP

ChIRP was performed as described by Chu et al. (2012) using the Magna ChIRP™ RNA Interactome Kit (Merck Millipore). ChIRP is based on affinity capture of target lncRNA and is applicable to many lncRNAs, as the design of affinity probes is straightforward, given an RNA sequence, requiring no prior knowledge of the structure of the RNA or its functional domains. ChIRP oligonucleotides were designed against PVT1 RNAs from each species using the Stellaris single-molecule FISH oligo designer (Biosearch Technologies) at http://single moleculefish.com. Antisense DNA probes with BiotinTEG at 3-prime ends were ordered. ChIRP oligonucleotides and pools are listed in Supplementary Tables S3 and S4. A total of 10 15-cm plates of PC cells were used per ChIRP experiment (100–500 million cells). Cell harvesting, lysis, disruption, and ChIRP were performed with several modifications. (i) Collected cells were cross-linked in 1% glutaraldehyde at room temperature for 10 min, followed by 0.125 M glycine quenching for 5 min, to preserve RNA–chromatin interactions before preparing cell pellets. (ii) DNA was sheared by sonicating the cross-linked cell lysates. Cell sonication was performed in a 4°C water bath at the highest setting (i.e. 30 sec ON, 45 sec OFF pulse intervals). (iii) Biotinylated DNA probes were hybridized to RNA and bound chromatin was isolated. RNA was extracted from ChIRP samples for qRT-PCR analysis.

Dual-luciferase reporter assays

The putative PVT1/HIF-1α promoter was amplified by PCR (Supplementary Table S7) and cloned into the *XhoI/HindIII* site of the pGL4-Control vector (Promega) to generate pGL4-PVT1-promoter and pGL4-HIF-1α-promoter vectors. All PCR products were confirmed by DNA sequencing. The 293T cells were transfected with pGL4-based constructs containing the PVT1/HIF-1α promoter and the Renilla luciferase plasmid (pRL-TK). Then, 293T cells (5×10^4) were seeded in 24-well plates 24 h before transfection. The following day, 30–100 ng of pGL4-PVT1-promoter or pGL4-HIF-1α-promoter reporter plasmids, along with NC siRNA and siHIF-1α/siPVT1 or along with vector adenovirus (vector) and overexpression adenovirus (oeHIF-1α/oePVT1), and 200 ng of internal control plasmids constitutively expressing Renilla luciferase were co-transfected using lipofectamine 2000 (Invitrogen). Cells were harvested 48 h post-transfection and evaluated for luciferase activity using a Dual-Luciferase Reporter Assay System (Promega). Each experimental trial involved cell transfection with the same plasmids in quadruplicate. Luciferase activity was normalized to the co-transfected pRL-TK plasmid (mean ± SD). These experiments were repeated at least three times and the *P*-value was calculated with two-tailed Student's *t*-test.

mRNA stability assay

HIF-1α or PVT1 expression was knocked down by siRNA transfection for 48 h. Then, *de novo* RNA synthesis was blocked by addition of 5 μg/ml actinomycine D (ActD; Apexbio) into the medium. Total RNA was harvested at indicated time points and mRNA expression was detected by qRT-PCR. Measurement of pre-ActD mRNA levels revealed mRNA half-life.

RNA extraction and qRT-PCR

Total RNA was isolated from treated cells with Trizol reagent (Invitrogen) and reverse-transcribed using a reverse transcription system to generate a cDNA template according to the manufacturer's instructions. qRT-PCR was performed using an SYBR green-containing PCR kit (TaKaRa) and an IQ5 sequence detection system (Applied Biosystems) according to the manufacturer's instructions. RNA input was normalized to the level of human GAPDH mRNA to determine relative gene expression. Primer sequences used for qRT-PCR are listed in Supplementary Table S6.

Western blotting

Whole-cell extracts were obtained by lysing cells in TNTE buffer (50 mM Tris, pH 7.4, 150 mM NaCl, 1 mM EDTA, 10 mM sodium pyrophosphate, 0.5% Triton X-100, 1 mM sodium vanadate, and 25 mM sodium fluoride) containing protease inhibitor (5 μg/ml PMSF). Protein samples were analyzed with monoclonal mouse anti-HIF-1α (Cell Signaling Technology, 1:1000) and mouse anti-β-actin (Sigma-Aldrich, 1:5000) antibodies. Quantity One software (Bio-Rad Laboratories) was used to quantify relative expression levels of target proteins.

Cell proliferation assay and cell clone formation assay

PANC-1 cells were first seeded on a 96-well plate at a density of 5×10^4 cells/ml and allowed to adhere in an incubator at 37°C and 5% CO_2 for 24 h. Eight hours after infection with recombinant adenovirus encoding HIF-1α or vector adenovirus, the HIF-1α-upregulated PANC-1 cells were transfected with PVT1 siRNA. Cell proliferation was measured after 24, 48, 72, and 96 h of incubation by adding 20 μl/well methyl tetrazolium salt (MTS) solution (Promega) for 4 h and measuring the absorbance at 490 nm. The cell density of each sample was calculated with a calibration curve plotted by OD against known cell numbers.

Cells were digested and 100 cells of each group were inoculated into a culture dish after cell infection and transfection treatment. Culture medium was changed every 2 days. Cell culture was performed for 2 weeks and was terminated when macroscopic apophyses were found in culture dishes. After washing with phosphate-buffered saline, fixation with 20% methanol for 15 min was performed. Then, an appropriate amount of Giemsa solution was added, and staining was performed for 40 min. After washing and air drying, clones were counted using a cloning counter.

Transwell migration assay, chamber invasion assay, and scratch wound-healing assay

For the transwell migration assay, 5×10^4 PANC-1 cells were plated on 8-μm Transwell filters (Corning). For the invasion assay, 1×10^5 cells were added to the upper chamber of each insert, coated with 150 μg Matrigel (BD Biosciences). The cells were induced to migrate toward medium containing 20% FBS for 24 h (for migration assay) and 48 h (for invasion assay) in the CO_2 incubator. Non-invading cells were removed with a cotton swab. The remaining cells were fixed and stained in dye solution containing 0.1% crystal violet and 20% methanol. The cells that had migrated or invaded were counted and imaged using an IX71 inverted microscope (Olympus Corp.). Ten random fields were chosen, and cell numbers were averaged.

For the scratch wound-healing assay, when the transfected/infected cells reached 80% confluence, a wound was created by scratching with a 200-μl pipette tip. After scratching, the detached cells were removed by washing twice and then the cells were maintained in fresh medium. Cells were imaged at 0 and 24 h after scratching, and the migration distance was calculated by measuring the width of the wound.

Xenograft tumorigenesis model

Four-week-old female BALB/c nude mice were purchased from Shanghai SLAC Laboratory Animal Co., Ltd. All mice were housed under standard housing conditions according to protocols approved by the Ethics Committee of Sir Run Shaw Hospital (Zhejiang, China), and the methods were carried out in accordance with the approved guidelines. All mice were divided into three groups randomly (Vector group, oeHIF-1α group, and oeHIF-1α+siPVT1 group), each group containing 5 mice. Nude mice were injected subcutaneously with 5×10^6 treated PANC-1 stable cells. Tumor volumes were calculated from the length (*a*) and the width (*b*) by using the following formula: volume (mm^3) $= a \times b^2/2$. Tumor volumes were calculated with calipers every week. Four weeks after injection, the animals were sacrificed by cervical dislocation in deep CO_2 anesthesia, and tumors were harvested (measured and weighed) and fixed in 4% paraformaldehyde or stored in −80°C with liquid nitrogen. Tumor weight was calculated as mean weight ± SD in each group.

Statistical analysis

All statistical analyses were performed using GraphPad Prism 5 software for Microsoft Windows. Student's *t*-test and one-way ANOVA were used to analyze two or multiple groups for statistical significance. Each experiment was performed in triplicate. Data were represented as mean ± SD. Western blotting, qRT-PCR, ChIP, ChIRP, and dual-luciferase reporter assay results represent three independent experiments. All tests were two-sided and *P*-values <0.05 were considered statistically significant.

Supplementary material

Funding

Conflict of interest: none declared.

References

Bhan, A., Soleimani, M., and Mandal, S.S. (2017). Long noncoding RNA and cancer: a new paradigm. Cancer Res. *77*, 3965–3981.

Chen, S., Chen, J.Z., Zhang, J.Q., et al. (2016). Hypoxia induces TWIST-activated epithelial–mesenchymal transition and proliferation of pancreatic cancer cells in vitro and in nude mice. Cancer Lett. *383*, 73–84.

Choudhry, H., Harris, A.L., and McIntyre, A. (2016). The tumour hypoxia induced non-coding transcriptome. Mol. Aspects Med. *47–48*, 35–53.

Chu, C., Qu, K., Zhong, F.L., et al. (2011). Genomic maps of long noncoding RNA occupancy reveal principles of RNA–chromatin interactions. Mol. Cell *44*, 667–678.

Chu, C., Quinn, J., and Chang, H.Y. (2012). Chromatin isolation by RNA purification (ChIRP). J. Vis. Exp. *61*, 3912.

Colombo, T., Farina, L., Macino, G., et al. (2015). PVT1: a rising star among oncogenic long noncoding RNAs. Biomed Res. Int. *2015*, 304208.

Cory, S., Graham, M., Webb, E., et al. (1985). Variant (6;15) translocations in murine plasmacytomas involve a chromosome 15 locus at least 72 kb from the c-myc oncogene. EMBO J. *4*, 675–681.

Cui, M., You, L., Ren, X., et al. (2016). Long non-coding RNA PVT1 and cancer. Biochem. Biophys. Res. Commun. *471*, 10–14.

Ding, J., Li, D., Gong, M., et al. (2014). Expression and clinical significance of the long non-coding RNA PVT1 in human gastric cancer. OncoTargets Ther. *7*, 1625–1630.

Du, S.C., Zhu, L., Wang, Y.X., et al. (2019). SENP1-mediated deSUMOylation of USP28 regulated HIF-1α accumulation and activation during hypoxia response. Cancer Cell Int. *19*, 4.

Erickson, L.A., Highsmith, W.E., Fei, P., et al. (2015). Targeting the hypoxia pathway to treat pancreatic cancer. Drug Des. Dev. Ther. *9*, 2029–2031.

Feng, J., Bi, C., Clark, B.S., et al. (2006). The Evf-2 noncoding RNA is transcribed from the Dlx-5/6 ultraconserved region and functions as a Dlx-2 transcriptional coactivator. Genes Dev. *20*, 1470–1484.

Gao, J., Aksoy, B.A., Dogrusoz, U., et al. (2013). Integrative analysis of complex cancer genomics and clinical profiles using the cBioPortal. Sci. Signal. *6*, pl1.

Grampp, S., Platt, J.L., Lauer, V., et al. (2016). Genetic variation at the 8q24.21 renal cancer susceptibility locus affects HIF binding to a MYC enhancer. Nat. Commun. *7*, 13183.

Görlach, A. (2009). Regulation of HIF-1α at the transcriptional level. Curr. Pharm. Des. *15*, 3844–3852.

Hansen, A.E., Kristensen, A.T., Law, I., et al. (2011). Hypoxia-inducible factors—regulation, role and comparative aspects in tumourigenesis. Vet. Comp. Oncol. *9*, 16–37.

Hidalgo, M. (2010). Pancreatic cancer. N. Engl. J. Med. *362*, 1605–1617.

Hon, W.C., Wilson, M.I., Harlos, K., et al. (2002). Structural basis for the recognition of hydroxyproline in HIF-1α by pVHL. Nature *417*, 975–978.

Huang, C., Yu, W., Wang, Q., et al. (2015). Increased expression of the lncRNA PVT1 is associated with poor prognosis in pancreatic cancer patients. Minerva Med. *106*, 143–149.

Huang, L.E. (2013). Biochemistry. How HIF-1α handles stress. Science *339*, 1285–1286.

Huang, T., Liu, H.W., Chen, J.Q., et al. (2017). The long noncoding RNA PVT1 functions as a competing endogenous RNA by sponging miR-186 in gastric cancer. Biomed. Pharmacother. *88*, 302–308.

Jin, L., Cai, Q., Wang, S., et al. (2020). Long noncoding RNA PVT1 promoted gallbladder cancer proliferation by epigenetically suppressing miR-18b-5p via DNA methylation. Cell Death Dis. *11*, 871.

Kapinova, A., Kubatka, P., Zubor, P., et al. (2018). The hypoxia-responsive long non-coding RNAs may impact on the tumor biology and subsequent management of breast cancer. Biomed. Pharmacother. *99*, 51–58.

Kapranov, P., Cheng, J., Dike, S., et al. (2007). RNA maps reveal new RNA classes and a possible function for pervasive transcription. Science *316*, 1484–1488.

Kim, T.H., and Dekker, J. (2018). Chromatin immunoprecipitation (ChIP) analysis of protein–DNA interactions. Cold Spring Harb. Protoc. *2018*, pdb.top082586.

Majmundar, A.J., Wong, W.J., and Simon, M.C. (2010). Hypoxia-inducible factors and the response to hypoxic stress. Mol. Cell *40*, 294–309.

Miller, K.D., Nogueira, L., Mariotto, A.B., et al. (2019). Cancer treatment and survivorship statistics, 2019. CA Cancer J. Clin. *69*, 363–385.

Min, J.H., Yang, H., Ivan, M., et al. (2002). Structure of an HIF-1α –pVHL complex: hydroxyproline recognition in signaling. Science *296*, 1886–1889.

Peng, J.F., Zhuang, Y.Y., Huang, F.T., et al. (2016). Noncoding RNAs and pancreatic cancer. World J. Gastroenterol. *22*, 801–814.

Semenza, G.L. (2001). HIF-1, O_2, and the 3 PHDs: how animal cells signal hypoxia to the nucleus. Cell *107*, 1–3.

Shih, J.W., Chiang, W.F., Wu, A., et al. (2017). Long noncoding RNA LncHIFCAR/MIR31HG is a HIF-1α co-activator driving oral cancer progression. Nat. Commun. *8*, 15874.

Shih, J.W., and Kung, H.J. (2017). Long non-coding RNA and tumor hypoxia: new players ushered toward an old arena. J. Biomed. Sci. *24*, 53.

Sun, Y.W., Chen, Y.F., Li, J., et al. (2014). A novel long non-coding RNA ENST00000480739 suppresses tumour cell invasion by regulating OS-9 and HIF-1α in pancreatic ductal adenocarcinoma. Br. J. Cancer *111*, 2131–2141.

Wang, L., Zhou, D., Tu, J., et al. (2014). Exploring the stability of long intergenic non-coding RNA in K562 cells by comparative studies of RNA–Seq datasets. Biol. Direct. *9*, 15.

Webb, E., Adams, J.M., and Cory, S. (1984). Variant (6;15) translocation in a murine plasmacytoma occurs near an immunoglobulin kappa gene but far from the myc oncogene. Nature *312*, 777–779.

Xie, Z., Chen, X., Li, J., et al. (2016). Salivary HOTAIR and PVT1 as novel biomarkers for early pancreatic cancer. Oncotarget *7*, 25408–25419.

Xu, M.D., Wang, Y., Weng, W., et al. (2017). A positive feedback loop of lncRNA-PVT1 and FOXM1 facilitates gastric cancer growth and invasion. Clin. Cancer Res. *23*, 2071–2080.

Yang, F., Huo, X.S., Yuan, S.X., et al. (2013). Repression of the long noncoding RNA-LET by histone deacetylase 3 contributes to hypoxia-mediated metastasis. Mol. Cell *49*, 1083–1096.

You, L., Chang, D., Du, H.Z., et al. (2011). Genome-wide screen identifies PVT1 as a regulator of gemcitabine sensitivity in human pancreatic cancer cells. Biochem. Biophys. Res. Commun. *407*, 1–6.

Yuen, A., and Díaz, B. (2014). The impact of hypoxia in pancreatic cancer invasion and metastasis. Hypoxia *2*, 91–106.

Zheng, R., Zeng, H., Zhang, S., et al. (2017). Estimates of cancer incidence and mortality in China, 2013. Chin J. Cancer *36*, 66.

Zhou, Q., Chen, J., Feng, J., et al. (2016). Long noncoding RNA PVT1 modulates thyroid cancer cell proliferation by recruiting EZH2 and regulating thyroid-stimulating hormone receptor (TSHR). Tumour Biol. *37*, 3105−3113.

Zhu, Z., Gao, X., He, Y., et al. (2012). An insertion/deletion polymorphism within RERT-lncRNA modulates hepatocellular carcinoma risk. Cancer Res. *72*, 6163−6172.

Zhuang, C., Li, J., Liu, Y., et al. (2015). Tetracycline-inducible shRNA targeting long non-coding RNA PVT1 inhibits cell growth and induces apoptosis in bladder cancer cells. Oncotarget *6*, 41194−41203.